Nanoarchitectonics
http://ojs.wiserpub.com/index.php/NAT/

Research Article

Stimulation of MSCs Osteogenic Differentiation on a Micro/Nanofibrous Scaffold Using Mechanical Stimulation in the Perfusion Bioreactor

Michala Rampichová[1*], Věra Hedvičáková[1,2], Erna Šljivnjak[1], Veronika Hefka Blahnová[1], Věra Sovková[1], Radmila Žižková[1,2], Matej Buzgo[1,3], Eva Filová[1]

[1]The Czech Academy of Sciences, Institute of Experimental Medicine, Videnska 1083, 14240, Prague, Czech Republic
[2]Technical University of Liberec, Studentska 1402/2, 461 17, Liberec 1, Czech Republic
[3]Biofabics Lda., Rua Alfredo Allen 455, 4200-135 Porto, Portugal
Email: michala.rampichova@iem.cas.cz

Received: 5 August 2022; **Revised:** 5 October 2022; **Accepted:** 18 October 2022

Abstract: In tissue engineering, the 3D constructs seeded with cells tested in vitro in static conditions suffer from poor cellular penetration and non-homogenous matrix deposition, due to the insufficient flow of nutrients, gases and signal molecules through the scaffold volume. However, a dynamic culture of cells can improve these drawbacks and simulate physiological conditions, such as flow in the canalicular system of bones. The purpose of this comparative study was to evaluate the different flow rates of 1 and 3 mL/min of perfusion bioreactor on human mesenchymal stromal cells (hMSCs), seeded in an osteogenic media on 3D porous constructs. After three weeks of dynamic cultivation, the metabolic activity and proliferation of the cells was evaluated, as well as the alkaline phosphatase (ALP) activity and the expression of bone related genes, RunX2, collagen type I and osteocalcin. The dynamic culture conditions did not influence the metabolic activity of hMSCs. The highest cell proliferation was detected on the scaffold cultured at a flow rate of 3 mL/min. The dynamic culture did not prove the penetration of cells into the scaffold's volume. The ALP activity, and PCR analysis of osteogenic markers RunX2 and collagen type I were highest on the scaffolds cultured at 1 mL/min, compared to the static culture and even to the dynamic culture at 3 mL/min. The study shows that hMSCs behave differently in different flow rates. While the higher flow rate (3 mL/min, shear stress 479 mPa) improved cell proliferation, the slower flow rate of 1 mL/min (shear stress 160 mPa) supported the ALP activity and expression of osteogenic marker genes. Interestingly, our expectation that dynamic culture improves cell penetration into the scaffold was not proved.

Keywords: perfusion, bioreactor, dynamic cultivation, mesenchymal stem cells, porous scaffold

1. Introduction

Tissue engineering aims to develop new fully functional tissue using artificial scaffolds, cells and/or bioactive molecules [1–3]. The formation of a new tissue is a complex process, where cells need to be stimulated by chemical and mechanical stimuli. In the human body, this process is controlled by growth factors, signalling pathways and the cell environment.

DOI: https://doi.org/10.37256/nat.5120244028

The induction of bone extracellular matrix formation in in vitro conditions is a complex task. However, successful osteogenic differentiation can be induced by the chemical stimulation of growth factors [4–6]. In addition to growth factors, many supplements have been tested and documented. Commonly used supplements for the osteogenic differentiation of cells are β-glycerol phosphate, dexamethasone and ascorbate-2-phosphate. The positive effect of these supplements on the osteogenic differentiation of mesenchymal stromal cells (MSCs) was documented in many studies [7, 8].

The mechanical stimulation of osteogenic differentiation can be performed using the dynamic culture conditions of cells that simulate the physiological requirements of the bone tissue. Dynamic culture conditions are induced by culture in bioreactors such as spinner flasks [9, 10], rotating wall bioreactors [10] and flow perfusion systems [11]. Extracellular fluid flow present in the bone canaliculi system, originates from mechanical loading and other stressors that have a physiological impact on bone tissue [12]. It was proved that perfusion flow enhances the formation of bone extracellular matrix and mineralization [13, 14]. Static culture conditions suffer from poor cell penetration of the scaffold volume, and non-uniform distribution of the nutrients, oxygen, regulatory molecules through the scaffold and the accumulation of metabolic products. As a consequence, the majority of the cell adhesion and distribution is concentrated on the outer surface of the scaffold, resulting in a non-homogenous matrix deposition.

Nanofibers and microfibers are popular materials among scaffolds for bone tissue engineering. The main reason is their high porosity with big interconnected pores, and fiber with a diameter that simulates molecules forming bone extracellular matrix [15]. The influence of fiber diameter and pore size of nano/microfibrous scaffolds was observed in our previous study [16]. Scaffolds prepared by the combination of melt-blown and electrospinning technology, combined nano- and microfibers, were the most appropriate for MSCs proliferation, infiltration into the scaffold and osteogenic differentiation.

In this study, we hypothesized that the process of osteogenic differentiation and cell adhesion and migration on the nano/microfibrous scaffolds, can be enhanced using mechanical stimulation from fluid flow generated by the perfusion bioreactor. Different perfusion flow rates on hMSCs cultured on three-dimensional (3D) scaffold for long-term were investigated. Enhanced cell proliferation and the infiltration of deep parts of the scaffold by hMSCs were estimated.

2. Methods

2.1 *Scaffold preparation*

Fibrous scaffolds were prepared from poly-ε-caprolactone (PCL, 45,000 Da; Sigma Aldrich), using technology combining melt-blown and electrospinning. The samples were prepared as previously described [16]. Briefly, a laboratory-scale melt-blown device (J&M Laboratories, USA) was combined with an electrospinning device (needleless wire spinner). The melt-blown technology used PCL pellets melted at temperatures 176, 250, 300, and 340 °F. The melt-blown extruder screw rotated at 7.5 rpm (100 g of polymer per 1 hour). The melt-blown die length was 75 mm with 60 orifices, each 0.4 mm in diameter. The distance of the melt-blown die from the collector was 600 mm. The fibers generated by electrospinning were mixed with melt-blown fibers by laminar airflow with a velocity 20 $m \cdot s^{-1}$. The spinner was situated at 300 mm distance from the melt-blown die, and at 300 mm distance from the drum collector. The drum collector rotated at 4 rpm. The electrospinning device with the wire electrode (diameter 30 mm, length 150 mm) rotated at 12 rpm. The roller was charged at 35 kV positive, and the collector charged at 15 kV negative. The experiment parameters were set at a temperature of 23 °C and relative humidity of 45%. The prepared fibrous layer was cut to round patches with 10 mm diameter, and sterilized for 30 min in 70% ethanol. Scaffolds were subsequently washed 3 times in a sterile phosphate buffer saline (PBS).

2.2 *Scanning electron microscopy*

The melt-blown samples were visualized using scanning electron microscopy (SEM). Samples were cut and stuck onto the holders, and coated with a thin layer of gold in a Quorum 150R S plus device (Quorum Technologies, Lewes, GB). Afterwards, the samples were visualized using SEM (Tescan, Vega, Brno, CZE). The mean fiber size, pore size and porosity were calculated in ImageJ software.

2.3 *Scaffold seeding*

The scaffolds were cut with a biopsy punch of a diameter 10 mm, placed in 48-well plate chambers and seeded with 5 × 106 human mesenchymal stem cells isolated from bone marrow (hMSCs; ScienCell, San Diego, California, USA) per sample in 100 µL of osteogenic differentiation medium: Minimal Essential Medium (MEM; Sigma Aldric), supplemented with 10% of fetal bovine serum (FBS; Sigma Aldrich), antibiotics (100 I.U./mL Penicillin, 100 µg/mL Streptomycin, Sigma Aldrich), 10 mM β-glycerol phosphate disodium salt (Sigma Aldrich), 100 nM dexamethasone (Medochemie) and 40 µg/mL ascorbic acid-2-phosphate (Sigma Aldrich). The cells were left to adhere for 2 hours in a CO_2 incubator. Subsequently, the cell seeded scaffolds were placed in the chambers of the perfusion bioreactor (OsteoGen, Instron; Figure 1) for dynamic culture (Dyn). Statically cultured scaffolds (Stat) were left in 48-well plates and 750 µL of medium was added. The medium in the static culture conditions was changed every 2 days.

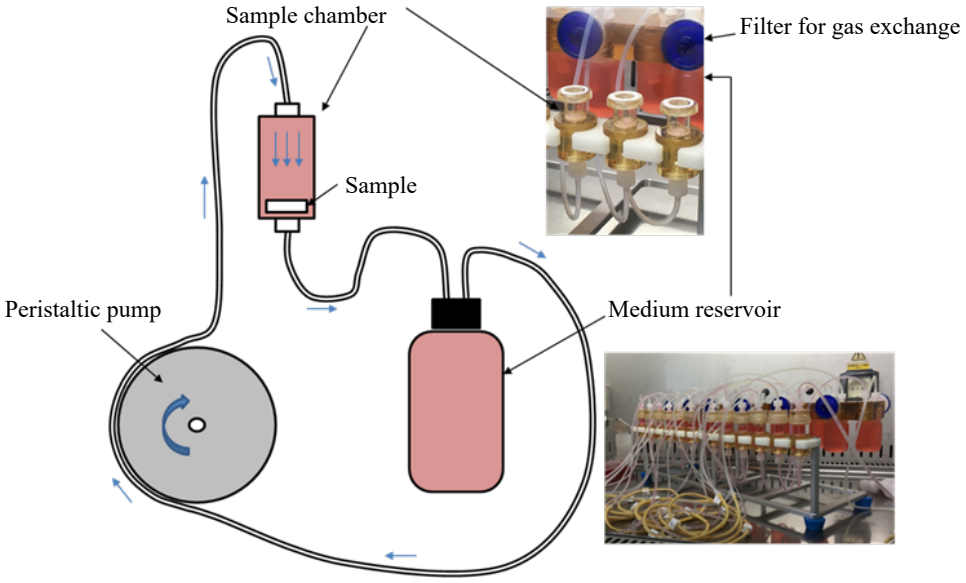

Figure 1. Schema of the bioreactor. The 12-sample bioreactor is composed of the sample chambers, medium reservoirs and peristaltic pump. The medium flowing from the medium reservoir is pushed out by a peristaltic pump to the sample chamber. The medium flows from the top of the chamber to output in the bottom of the chamber, and continues by the tube to the medium reservoir. The components of the bioreactor form a closed sterile system, gas exchange is provided by sterile filters. The whole bioreactor is placed in an incubator, providing a temperature of 37 °C and 5% of CO_2.

2.4 *Dynamic culture in the perfusion bioreactor*

A perfusion bioreactor was used for dynamic culture. Cell seeded scaffolds were placed in the individual chambers of the bioreactor. The diameter of the bioreactor chambers was 10 mm, so, the scaffolds fit well in the chambers. The system was filled with a medium using reverse flow. 30 mL of differentiation medium circulated in the system. The perfusion rate was set at 1 or 3 mL/min. The experiment was ended after 21-day incubation, when the tests of cell proliferation and osteogenic differentiation were performed. Cell seeded scaffolds cultured in static conditions in a 48-well plate were used as a control for all analyses. The static control was seeded for every flow rate run of the bioreactor. As the hMSCs are primary cells, the data slightly differed across the static controls. For this reason, the data from the following analysis (MTS, DNA quantification, ALP activity) measured for dynamic conditions, were related to data measured for static conditions in every run. The values measured for dynamic cultures were divided by the average value of corresponding static culture.

2.5 *Calculation of shear stress*

The calculation of shear stress (τ) was based on the publication of Hadida and Marchat [17]:

$$\tau \cong \frac{8 \cdot \mu \cdot Q}{d \cdot A \cdot p}$$

where μ is liquid dynamic viscosity, Q is flow rate, d is pore diameter, A is cross-section of the scaffold and p is porosity percentage. The value of the medium dynamic viscosity was measured using rheometer (Anton Paar) at 50% of shear rate and was determined as 0.83 ± 0.03 mPa·s.

2.6 *Cell viability analysis*

MTS assay (CellTiter 96® AQueous One Solution Cell Proliferation Assay; Promega) was used to probe cell metabolic activity. Dynamically cultured samples (5 independently samples per group) were transferred to the wells of a 48-well plate, statically cultured samples were moved to clean wells to avoid the measurement of cells growing on the bottom of the wells. MTS solution (80 µL) was added to 400 µL of the medium containing only FBS and antibiotics. The microplate was incubated at 37 °C for 2 hours. The absorbance of the solution (100 µL) was read in clean microplates using microplate reader (Infinite M200 PRO, Tecan, Switzerland) at 490 nm, and reference wavelength 690 nm.

2.7 *Analysis of cell proliferation*

The quantification of DNA was used as a measure for determination of cellular proliferation. The samples were analysed using the PicoGreen method (Quant-iT^{TM} dsDNA Assay Kit; Life Technologies). The scaffolds (5 independently cultured samples) were lysed by freeze-thawing (3 cycles with rough vortexing) in 400 µL of cell lysis solution (0.2% *v*/*v* Triton X-100, 10 mM Tris (pH 7.0), and 1 mM EDTA). For analysis, 10 µL of samples was added to 200 µL of PicoGreen reagent solution. The fluorescence intensity was recorded on multimode fluorescence reader (Infinite M200 PRO, Tecan, Switzerland; λ_{ex} = 485 nm, λ_{em} = 523 nm). The results were evaluated using the calibration curve of the standards in the kit.

2.8 *Visualization of cell distribution in scaffolds*

The cell distribution in the fibrous scaffolds was detected using confocal microscopy. The samples were fixed with frozen methyl alcohol (−20 °C) for 10 min. Subsequently, the fluorescent probe 3,3′-diethyloxacarbocyanine iodide (DiOC6(3); Invitrogen, 1 µg/mL in PBS, pH 7.4) was added and incubated with the samples for 45 min at room temperature, to visualize the intercellular membranes. Subsequently, cell nuclei were stained using propidium iodide (PI; Sigma Aldrich, 5 µg/mL in PBS, 10 min). The scaffolds were washed with PBS, and visualized using confocal microscopy (ZEISS LSM 5 DUO, PI: λ_{ex} = 561 nm, λ_{em} = 630–700 nm; DiOC6(3): λ_{ex} = 488 nm, λ_{em} = 505–550 nm). The images from propidium iodide staining were subsequently process into color-coded projections. The color of the cell nuclei of each depth section corresponds to the color on the scale. The samples used for confocal microscopy were afterwards used for SEM visualization. The samples were dehydrated using ethanol solutions with increasing concentration (35, 48, 70, and 96%). Subsequently, a few drops of hexamethyldisilazane (Sigma Aldrich) were added, and the samples were left to air dry at room temperature. The prepared samples were coated with gold and visualized using SEM as was described in Section 2.2.

2.9 *Detection of alkaline phosphatase activity*

The activity of alkaline phosphatase (ALP) was measured using 1-Step^{TM} PNPP kit (Thermo Scientific, USA). 4 independently cultured samples were used for measurement of ALP activity. PNPP reagent (350 µL) was added to the samples and incubated for 10 min at room temperature. The reaction was stopped by adding 2N NaOH (175 µL). The absorbance of the samples was recorded by microplate reader at 405 nm (Infinite M200 PRO, Tecan, Switzerland).

2.10 *RNA isolation and qPCR analysis*

The total RNA was isolated using the Qiagen RNA mini-kit (Qiagen, Hilden, Germany) from 3 independently cultured samples, according to the protocol provided by the manufacturer. RNA concentration was measured using

NanoQuant Plate (Tecan) and reader Infinite M200 PRO, the ratio of wavelengths 280/260 nm was measured for purity evaluation. Reverse transcription (RT) was performed using the RevertAid First Strand cDNA Synthesis Kit (ThermoFisher Scientific, Waltham, MA, USA) with 80 ng of the total RNA. Transcript levels were evaluated using quantitative PCR (qPCR). qPCR was performed using the Light Cycler 480 Roche (Roche, Basel, Switzerland). To each reaction, TaqMan™ Gene Expression Master Mix (4369016, Life Technologies), PCR Grade Water and TaqMan Gene Expression Assay, containing both primers and probe, were added. List of assays used: eukaryotic translation elongation factor 1 alpha 1 (EEF1A1, Hs00265885_g1) as a housekeeping gene, RunX2 (Hs01047973_m1), collagen type I (COL1) (Col1A1, Hs00164004_m1) and osteocalcin (OCN) (BGLAP, Hs01587814_g1), all ThermoFisher Scientific. The thermo cycling parameters of qPCR were: activation 95 °C, 10 min; amplification 95 °C for 10 s, 60 °C for 10 s (45 cycles); termination 40 °C for 1 min. The data were evaluated using the relative quantification $2^{-\Delta Ct}$) method, for each gene relative to the endogenous control gene EEF1A1.

2.11 *Statistical analysis*

Quantitative data are presented as mean values ± standard deviation (SD). The averaged values were determined from 5 independently prepared samples for metabolic activity analysis and DNA quantification, 4 samples for detection of ALP activity and 3 samples for qPCR analysis. The results were evaluated statistically using SigmaStat 12.0, Systat. The normality of the data was tested by Kolmogorov-Smirnov test. The equality of variances was tested using Levene's test. If the data passed the normality test and the test of equality of variances, the statistical significance between a pair of groups was determined by ANOVA test and Tukey's comparative test for post-hoc analysis. If the data were without normal distribution, the statistical significance between a pair of groups was determined using Kruskal-Wallis test and Dunn's multiple comparisons test, for post hoc analysis. All the results were considered statistically significant if p was <0.05.

3. Results

3.1 *Characterization of scaffolds*

The micro/nanofibrous scaffolds were prepared by the hybrid spinning method, resulting in the formation of a composite mesh containing melt-blown microfibers and electrospun nanofibers (Figure 2). The analysis of morphology showed that the melt-blown fibers had a mean diameter of 9.8 ± 5.9 µm. The microfibers formed the main network of the scaffold, resulting in the formation of a 3D mesh. The electrospun nanofibers formed a looser network filling the pores in melt-blown fibers. The electrospun fibers had a mean diameter of 719 ± 118 nm. The SEM images (Figure 2) also showed a high compaction level of the scaffold, decreasing the total pore size. The mean pore size was 69.7 ± 31.1 μm^2. However, larger pores reaching even 1450 μm^2 were detected in some areas of the composite scaffold structure.

3.2 *Cell culture in bioreactors*

The scaffolds were placed in bioreactor chambers. A tight fit was guaranteed by using samples slightly larger than the reactor chambers, and their fitting resulted in perfusion flow through the scaffold. The cells were seeded on the scaffolds and cultured under different flow rates. The shear stress for the scaffold with diameter of 10 mm, pore size 69.7 μm^2, porosity 94% and the dynamic viscosity of the medium 0.83 mPa·s and the flow rates 1 and 3 mL/min was calculated as 160 and 479 mPa respectively.

3.3 *Cell metabolic activity and proliferation*

The metabolic activity of hMSCs cultured in static and dynamic conditions was measured after 21-days culture. As shown on Figure 3A, there were no differences in the metabolic activity of cells cultured in static and dynamic conditions, at any of tested flow rates.

Different results were observed in the cell proliferation tests, measured as the quantification of DNA on day 21 (Figure 3B). The highest proliferation was detected at flow rate 3 mL/min. Cell proliferation at 3 mL/min was

statistically higher than static culture and dynamic culture at 1 mL/min.

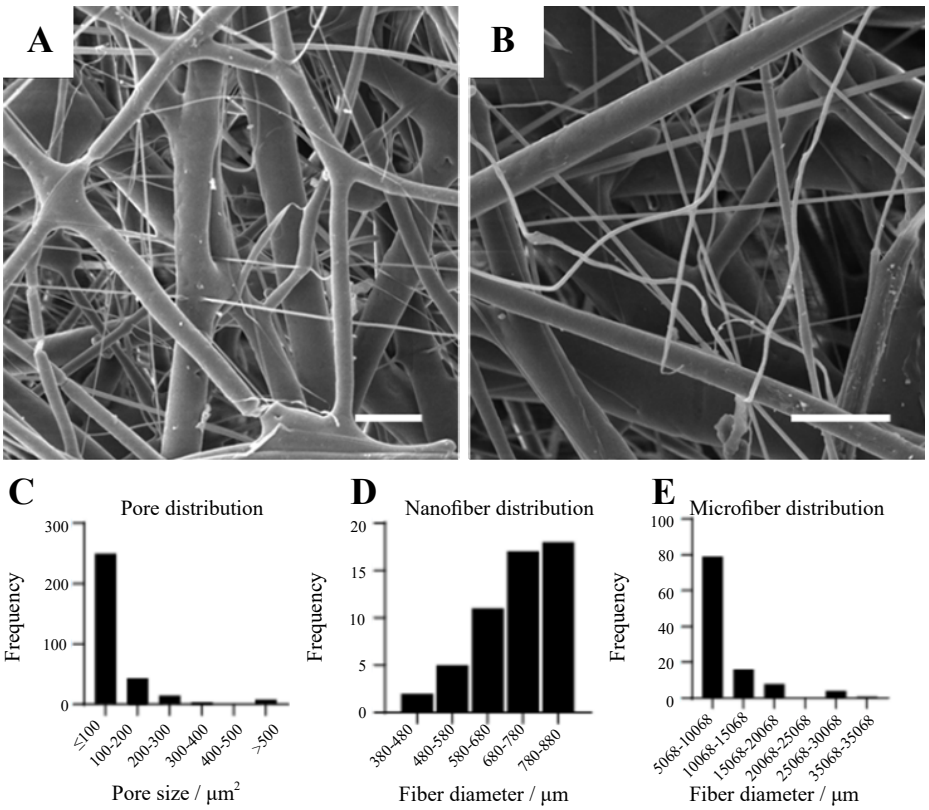

Figure 2. The process of melt-blown in combination with electrospinning, resulted in a micro/nanofibrous structure of the scaffold. The morphology of the scaffold was visualized using scanning electron microscopy (SEM). Magnification 3000× (A) and 2000× (B), scale 20 µm. The histograms show distribution of pore size (C), nanofibers (D) and microfibers (E).

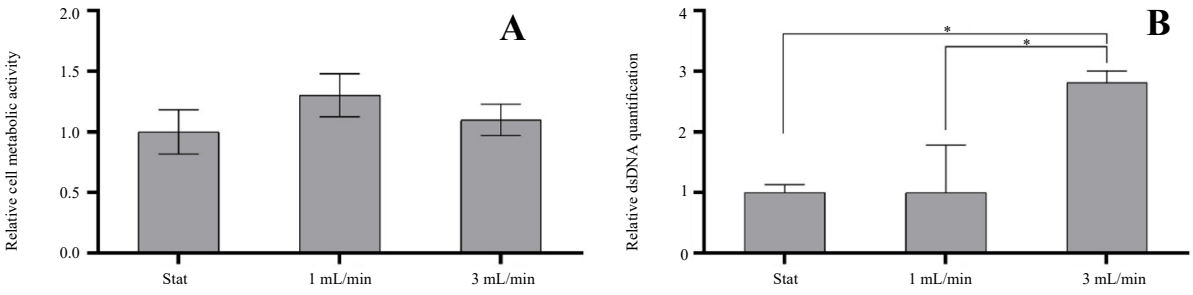

Figure 3. hMSCs metabolic activity and proliferation on day 21. Cell metabolic activity was measured using MTS test (A), cell proliferation was measured using DNA quantification kit (B). Data are related to data measured for static culture. *$p < 0.05$

Cell distribution on scaffolds was observed by confocal microscopy (Figure 4) and SEM (Figure 5) 21 days after seeding. The cells covered the whole surface of the scaffolds confluently. Confocal microscopy showed a dense cell layer, which was formed on the surface of the scaffolds, cultured in both static and dynamic conditions. Interestingly, the penetration of cells was comparable on all scaffolds, whether cultured in static or dynamic conditions, and reach only 90–100 µm. Similar results brought visualization by SEM. The dense layer of cells covered the fibrous scaffolds.

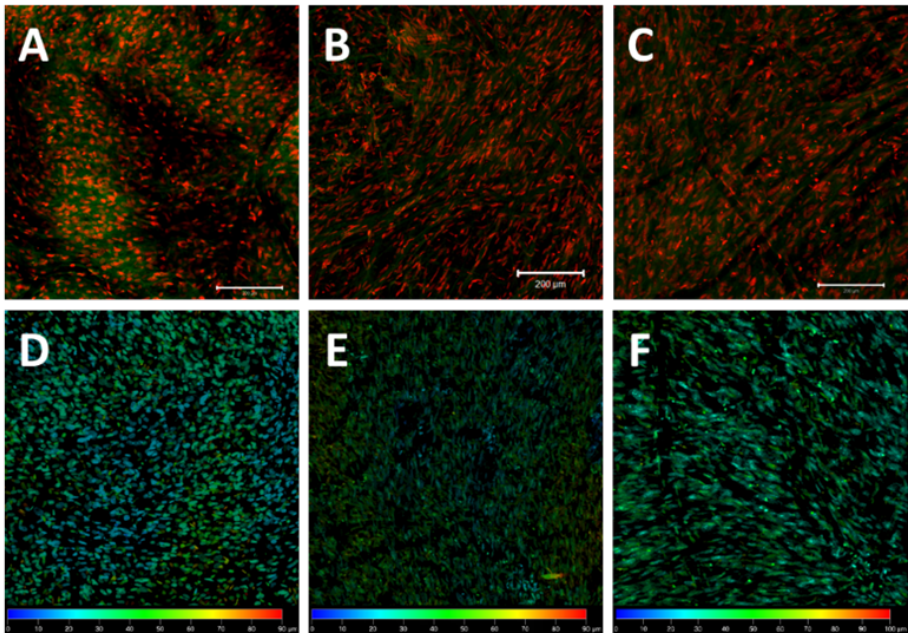

Figure 4. Cell distribution on scaffold visualized using confocal microscopy 21 days after seeding on scaffolds cultured in static conditions (A), dynamic conditions at 1 mL/min (B), and 3 mL/min (C) respectively. Cell intracellular membranes were stained using DiOC6(3) (green color), cell nuclei using propidium iodide (red color). The single sections of propidium iodide staining were assembled and a color-coded projection was created. The color of nuclei corresponds to the depth on the scale. It is visible that penetration of cells in the samples cultured in static (D) or dynamic conditions at 1 mL/min (E) or 3 mL/min (F) are comparable and reach only 90–100 µm. Scale 200 µm

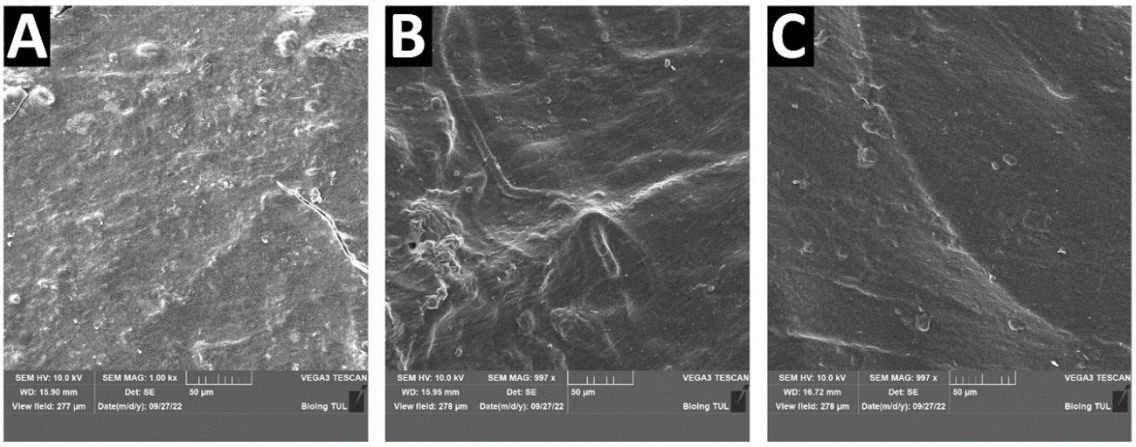

Figure 5. Visualization of cells cultured on fibrous scaffolds using SEM after 21 days of culture in static (A) and dynamic conditions at 1 mL/min (B), and 3 mL/min (C), respectively. The hMSCs formed dense layers in all groups and covered the whole surface of the fibrous scaffolds

3.4 *Osteogenic differentiation of hMSCs*

After three weeks of cultivation, the influence on osteogenic differentiation of hMSCs by different flow rates was detected using the quantification of ALP activity and qPCR analysis. The highest ALP activity was detected when a flow rate of 1 mL/min was applied (Figure 6A). The ALP activity of cells cultured at a flow rate of 3 mL/min was comparable with the statically cultured cells. Using qPCR we analysed the expression of bone related genes, namely RunX2, COL1 and OCN (Figure 6B–D). The expression of all the tested genes was detected in both the static and dynamic culture conditions, as both culture conditions used osteogenic differentiation media. The expression of RunX2 and COL1 mRNA was highest for the cells cultured at a flow rate of 1 mL/min. The cells cultured at a flow rate of 3 mL/min showed the expression of these markers similar to the statically cultured cells. The statistical analysis did not prove

a difference in the expression of OCN mRNA between any of the dynamic and static cultures, due to a large standard deviation, however, the trend observed is similar to other osteogenic marker assays, the dynamic culture at 1 mL/min resulted in a higher relative expression of OCN gene.

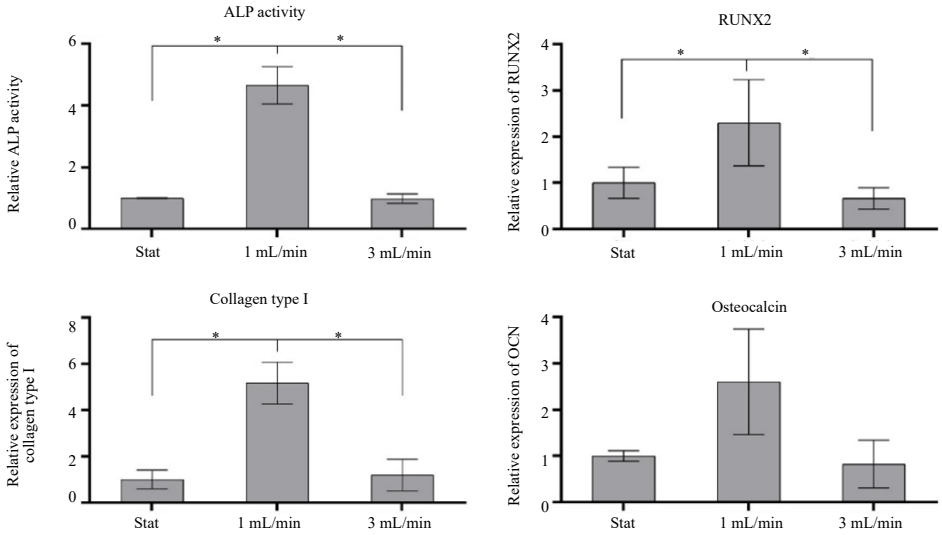

Figure 6. Osteogenic differentiation of hMSCs was detected using ALP activity measurement and qPCR analysis of osteogenic markers after 21 days of cultivation. ALP activity was measured by 1-Step™ PNPP kit. (A). Relative expression of RunX2 (B), COLI (C) and OCN (D) were determined by qPCR analysis, EEF1A1 was used as a housekeeping gene. Data were related to static control. *$p < 0.05$

4. Discussion

The scaffolds prepared using a combination of melt-blown technology and electrospinning showed very good results in vitro, when compared with the scaffolds prepared using classic electrospinning and electro-blowing [16]. The melt-blown scaffold has pore diameter of a maximum size of 68.8 µm, while the maximum pore size of the electrospun scaffold was 7.24 µm, and 24.13 µm for the scaffold prepared using electro-blowing. The pores of the melt-blown scaffold were big enough to enable cell penetration to the depth of the scaffold, and showed a higher proliferation and expression of osteogenic markers, compared to the other tested scaffolds. The success of the scaffold was connected with the highest pore size, compared to the scaffolds prepared using electrospinning and electro-blowing. Nanofibers prepared using electrospinning are well known to support adhesion of different cell types [18, 19]. This is ascribed to submicron dimensions of nanofibers, which correspond to dimensions of extracellular matrix fibers. On the other hand, limitations of these layers lie in its sheet structure and poor mechanical properties. In our study, combination of electrospun fibers with microfibers prepared using melt-blown technology provided increased porosity and 3-dimensionality, which is essential in bone tissue engineering applications.

In this study, we hypothesized that the culture of the scaffold in the perfusion bioreactor will simulate the in vivo conditions of bone tissue, and stimulate hMSCs to infiltrate the scaffolds and differentiate in osteoblasts more efficiently. hMSCs were seeded on the scaffolds in the perfusion bioreactor at a different fluid flow, 1 mL/min and 3 mL/min respectively, and we compared them to the statically cultured scaffolds.

Recently, the relevance of flow rate, as an indicator of the dynamic culture effect on cells, has been questioned. The reason for this is that the morphology of the scaffold, its porosity and pore size and viscosity of the medium, has to be taken into consideration [17]. The shear stresses calculated for the tested fluid flows in our study at rates of 1 and 3 mL/min are, in the case of our scaffold, 160 and 479 mPa respectively. Nevertheless, most of the published studies discuss flow rate as an only indicator. The values of the shear stress were calculated for the discussed studies, where all the necessary data were published and are presented in the following text next to flow rate values.

In our study, the perfusion flow had no effect on the cell metabolic activity measured using the MTS test. The measured values were comparable when cultured in the static or any of the dynamic conditions. On the other hand, the influence of the dynamic culture on cell proliferation was evident. The highest increase in the cell number was measured

on the scaffold cultured at a flow rate of 3 mL/min.

The results of the metabolic activity and proliferation from published studies are ambiguous. Bancroft, et al. used the flow perfusion culture system, flow rates of 0.3, 1 and 3 mL/min (shear stress 2.01, 6.73, and 20.14 mPa·s respectively), for a 3D titanium fiber mesh scaffold, seeded with rat marrow stromal osteoblasts cultured for 16 days [14]. They detected no differences in the DNA quantification between static and dynamic conditions, however histological sectioning of the scaffold showed increased cell penetration into the volume of the scaffold with an increasing flow rate. Similarly, no increase in the DNA amount was detected when rat bone marrow stromal cells (rBMSCs) were cultured in osteogenic differentiation media on a 3D titanium porous mesh for 16 days at a flow rate of 0.3 mL/min [20]. In some studies, the enhancement of metabolic activity was only detected for some flow rates. For example, Su et al. seeded an MG-63 osteosarcoma cell line on a 3D porous chitosan scaffold, and cultured them in perfusion dynamic conditions with flow rates of 0.24, 0.48 and 0.72 mL/min (shear stresses 5.9, 11.8, and 17.7 mPa·s respectively) for 21 days. The enhanced metabolic activity was proved for the flow rate of 0.24 mL/min, the higher flow rates were comparable with the static culture conditions [21]. On the other hand, in other studies, the dynamic culture of cells on the scaffolds proved better cell metabolic activity, proliferation and distribution inside the scaffold. Gomes, et al., seeded a starch-based scaffold with rBMSCs, and cultured them in an osteogenic differentiation media at a flow rate of 0.3 and 1 mL/min for 16 days. The higher flow rate induced an increase in cell number, and improved distribution of the cells within the scaffold [22]. Du et al. tested the porous tricalcium phosphate scaffold seeded with a mouse osteoblast such as MC3T3E1 cell line, and incubated them in a flow rate of 1 mL/min for 6 days. They observed a higher DNA amount and better penetration of the scaffold by the cells in the dynamically cultured conditions [23]. Fassina et al. incubated a Saos2 osteosarcoma cell line on a polyurethane foam in a flow of 3 mL/min for 16 days. They detected better distribution of the cells within the scaffold under dynamic culture conditions [24]. Sikavitsas et al. seeded rBMSCs in an osteogenic differentiation media on a 3D titanium porous mesh for 16 days in dynamic conditions, with a flow rate of 0.3 mL/min. They revealed an enhanced distribution of cells in the volume of the scaffold [20].

In this study, the cell penetration was very low, only 90–100 μm, and was not improved by the dynamic culture at any of the tested flow rates. The penetration was also lower compared to previous in vitro experiments [16], where cells penetrated in a depth of at least 250 μm inside the scaffold, even in the static culture. The stereological analysis showed a smaller pore size (maximum pore diameter was 21.5 μm in the present study in contrast to 68.8 μm in the previous study). The smaller pore size in the present study was caused by the increased fraction of nanofibers (in previous it was 9% and in the current scaffolds ~50%) resulting in a higher interlayer density. The density might have a negative impact on cell penetration to the scaffold. In addition, the difference was also shown in the process of cell seeding. The cells were seeded in high density, with the aim of fast reaching of osteogenic differentiation. It is known that hMSCs undergo osteogenic differentiation when they reach confluence [25]. Therefore, it is beneficial to use high seeding density to shorten the proliferative period of the cells before reaching confluency. In this study, cell seeding density was 4.7-fold higher compared to the previous study (6.37×10^6 current study vs. 1.35×10^6 cells/cm^2 in previous study). Cells were seeded on the scaffolds and left to adhere for 2 hours to prevent wash out from the scaffold by the medium flow. The seeding density was so high that the cells most likely interact with each other, preferably on the scaffold surface, and create a tough layer. A better strategy is probably to infiltrate the scaffold before cell adhesion by the process of dynamic cell seeding. The seeding can be done by perfusion [26, 27], oscillatory flow [28], centrifugal seeding [29], rotating cell seeding [30], stirred seeding in spinner flasks [31], hydrodynamic loading seeding [32] or by agitation [31]. Koch, et al. tested the effect of different perfusion velocities, and the number of perfusion cycles on seeding efficiency [28]. They show that cell seeding efficiency was rather influenced by the number of the perfusion seeding cycles. On the other hand, the perfusion cell seeding efficiency was comparable to the static cell seeding, when the cells were injected inside the scaffold. The perfusion seeding results in a more uniform cell distribution.

The osteogenic differentiation of hMSCs cultured in dynamic conditions was detected as ALP activity, and the expression of specific markers of osteogenic differentiation, namely RunX2, COL1 and OCN. The ALP activity and even the expression of RunX2 and COL1, were highest on the scaffolds cultured at 1 mL/min, when compared to the static and even dynamic culture at 3 mL/min.

Most of the published studies present enhanced osteogenic differentiation of cells cultured in dynamic conditions. In the study of Bancroft et al., the ALP activity of cells cultured in the static condition was lower compared to dynamic conditions, no differences were revealed between the flow rates of 0.3, 1 and 3 mL/min (shear stress 2.01, 6.73, and

20.14 mPa·s respectively). They also revealed an increase in mineralized matrix deposition with increasing flow rate. The secretion of osteopontin was comparable between all the culture conditions [14]. Fassina et al. incubated a Saos2 osteosarcoma cell line on a polyurethane foam at a flow rate of 3 mL/min for 16 days. They detected higher COL1, osteopontin and OCN secretion and calcium deposition [24]. In the study of Su et al., they showed an enhanced ALP activity on the MG-63 cells cultured at a flow rate of 0.24 mL/min (shear stress 5.9 mPa·s), higher flow rates of 0.48 (shear stress 11.8 mPa·s) and 0.72 mL/min (shear stress 17.7 mPa·s) were comparable with the static culture conditions. An improved mineral deposition and cell distribution within the scaffold was observed on the dynamically cultured scaffolds [21]. In some studies, no difference in ALP activity between the static and dynamic conditions was detected [23].

Most of the published studies worked with flow rates up to 3 mL/min. In the studies where more flow rates were compared, similar results were described for the different flow rates [14]. On the other hand, better results for lower flow rates in the sense of cell proliferation, and even osteogenic differentiation, compared to the higher flow rates have been published [21]. In this study, the flow rates of 1 and 3 mL/min were compared. Although the flow rates are in the range of commonly used values, the shear stress were higher than in the compared studies thanks to small pore size. It was shown that the lower flow rate of 1 mL/min (shear stress 160 mPa·s) supported the osteogenic differentiation of hMSCs, while the flow rate of 3 mL/min (shear stress 479 mPa·s) supported cell proliferation.

A further issue of the successful dynamic culture of cells on scaffolds in perfusion bioreactors is its design, direction of the flow and the mixing of the culture medium. Many commercial systems, as well as self-constructed bioreactor systems, were described in the literature. Based on the design, the flow of the media through the scaffolds can differ. The mixing of the culture media on the outer surface as well as inside the scaffold, is a major drawback of most systems. Olivier et al. dealt with the influence of flow direction on cells cultured in a large bone construct. They tested convergent and divergent flow. The convergent direction of the flow was found to be more efficient in terms of glucose consumption, cell proliferation and OCN expression [32]. Du et al. tested porous tricalcium phosphate scaffolds, seeded with a mouse osteoblast such as MC3T3E1 cell line, either in unidirectional flow rate of 1 mL/min or in an oscillatory perfusion culture system with flow rates of 0.5 and 1 mL/min for 6 days. In oscillatory conditions, they observed a homogenous distribution of cells in the volume of the scaffold. The amount of DNA was higher when the cells were cultured under unidirectional flow. Improved ALP activity was detected under the oscillatory flow rate of 0.5 mL/min [23]. In this study, we used unidirectional flow. The application of oscillatory flow can be used for the further enhancement of dynamic culture results.

5. Conclusions

We can conclude that hMSCs behaved differently in different flow rates. While the higher flow rate (3 mL/min) improved cell proliferation, the slower flow rate of 1 mL/min, corresponding to a shear stress of 68 mPa, supported osteogenic differentiation. Interestingly, our expectation that a dynamic culture improves cell penetration into the scaffold was not proved. The success of the dynamic culture most likely lies in the cell seeding mechanism. Dynamic cell seeding and the application of oscillatory flow, will be the next direction of our dynamic culture studies.

Acknowledgments

This study was supported by the Czech Science Foundation grant no. 18-09306S and Czech Health Research Council, grant no. NV18-05-00379, and by EU Horizon 2020 MSCA-RISE-2018 Research and Innovation Staff Exchange Program, project iP-OSTEO “Induced pluripotent stem cell for bone and cartilage defects” under the Marie Skłodowska-Curie grant agreement No 824007. We would like to kindly thank to Jiří Chvojka and Jakub Erben from the Technical University of Liberec for the provision of melt-blown fibrous scaffolds.

Conflict of interest

The authors declare no conflict of interest.

References

[1] Rustom LE, Boudou T, Nemke B, Lu Y, Hoelzle DJ, Markel MD, Picart C, Johnson AJW. Multiscale Porosity Directs Bone Regeneration in Biphasic Calcium Phosphate Scaffolds. *ACS Biomaterials Science & Engineering*. 2016; 3: 2768-2778. Available from: https://doi.org/10.1021/acsbiomaterials.6b00632.

[2] Bouyer M, Guillot R, Lavaud J, Plettinx C, Olivier C, Curry V, Boutonnat J, Coll JL, Peyrin F, Josserand V, et al. Surface delivery of tunable doses of BMP-2 from an adaptable polymeric scaffold induces volumetric bone regeneration. *Biomaterials*. 2016; 104: 168-181. Available from: https://doi.org/10.1016/j.biomaterials.2016.06.001.

[3] Fernandez-Bances I, Perez-Basterrechea M, Perez-Lopez S, Batalla DN, Rodríguez MAF, Alvarez-Viejo M, Ferrero-Gutierrez A, Menendez-Menendez Y, Garcia-Gala JM, Escudero D, et al. Repair of long-bone pseudoarthrosis with autologous bone marrow mononuclear cells combined with allogenic bone graft. *Cytotherapy*. 2013; 15: 571-577. Available from: https://doi.org/10.1016/j.jcyt.2013.01.004.

[4] Reible B, Schmidmaier G, Moghaddam A, Westhauser F. Insulin-Like Growth Factor-1 as a Possible Alternative to Bone Morphogenetic Protein-7 to Induce Osteogenic Differentiation of Human Mesenchymal Stem Cells in Vitro. *International Journal of Molecular Sciences*. 2018; 19: 1674. Available from: https://doi.org/10.3390/ijms19061674.

[5] Demirtaş TT, Göz E, Karakeçili A, Gümüşderelioğlu M. Combined delivery of PDGF-BB and BMP-6 for enhanced osteoblastic differentiation. *Journal of Materials Science - Materials in Medicine*. 2015; 27: 1-11. Available from: https://doi.org/10.1007/s10856-015-5626-9.

[6] Aksel H, Huang GTJ. Combined Effects of Vascular Endothelial Growth Factor and Bone Morphogenetic Protein 2 on Odonto/Osteogenic Differentiation of Human Dental Pulp Stem Cells In Vitro. *Journal of Endodontics*. 2017; 43: 930-935. Available from: https://doi.org/10.1016/j.joen.2017.01.036.

[7] Lukasova V, Buzgo M, Vocetkova K, Kubikova T, Tonar Z, Doupnik M, Blahnova V, Litvinec A, Sovkova V, Voltrova B, et al. Osteoinductive 3D scaffolds prepared by blend centrifugal spinning for long-term delivery of osteogenic supplements. *RSC Advances*. 2018; 8: 21889-21904. Available from: https://doi.org/10.1039/c8ra02735h.

[8] Brauer A, Pohlemann T, Metzger W. Osteogenic differentiation of immature osteoblasts: Interplay of cell culture media and supplements. *Biotechnic & Histochemistry*. 2016; 91, 161-169. Available from: https://doi.org/10.3109/10520295.2015.1110254.

[9] Mygind T, Stiehler M, Baatrup A, Li H, Zou X, Flyvbjerg A, Kassem M, Bünger C. Mesenchymal stem cell ingrowth and differentiation on coralline hydroxyapatite scaffolds. *Biomaterials* 2007; 28, 1036-1047. Available from: https://doi.org/10.1016/j.biomaterials.2006.10.003.

[10] Sikavitsas VI, Bancroft GN, Mikos AG. Formation of three-dimensional cell/polymer constructs for bone tissue engineering in a spinner flask and a rotating wall vessel bioreactor. *Journal of Biomedical Materials Research.* 2002; 62: 136-148. Available from: https://doi.org/10.1002/jbm.10150.

[11] Bjerre L, Bünger CE, Kassem M, Mygind T. Flow perfusion culture of human mesenchymal stem cells on silicate-substituted tricalcium phosphate scaffolds. *Biomaterials*. 2008; 29: 2616-2627. Available from: https://doi.org/10.1016/j.biomaterials.2008.03.003.

[12] Fritton SP, McLeod KJ, Rubin CT. Quantifying the strain history of bone: spatial uniformity and self-similarity of low-magnitude strains. *Journal of Biomechanics*. 2000; 33: 317-325. Available from: https://doi.org/10.1016/S0021-9290(99)00210-9.

[13] Bouet G, Cruel M, Laurent C, Vico L, Malaval L, Marchat D. Validation of an in vitro 3D bone culture model with perfused and mechanically stressed ceramic scaffold. *eCells and Materials Journal*. 2015; 29: 250-267. Available from: https://doi.org/10.22203/ecm.v029a19.

[14] Bancroft GN, Sikavitsas VI, Van Den Dolder J, Sheffield TL, Ambrose CG, Jansen JA, Mikos AG. Fluid flow increases mineralized matrix deposition in 3D perfusion culture of marrow stromal osteoblasts in a dose-dependent manner. *Proceedings of the National Academy of Sciences*. 2002; 99: 12600-12605. Available from: https://doi.org/10.1073/pnas.202296599.

[15] Lukášová V, Buzgo M, Vocetková K, Sovková V, Doupník M, Himawan E, Staffa A, Sedláček R, Chlup H, Rustichelli F, Amler E. Needleless electrospun and centrifugal spun poly-ε-caprolactone scaffolds as a carrier for platelets in tissue engineering applications: A comparative study with hMSCs. *Materials Science and Engineering: C*. 2019; 97: 567-575. Available from: https://doi.org/10.1016/j.msec.2018.12.069.

[16] Rampichová M, Chvojka J, Jenčová V, Kubíková T, Tonar Z, Erben J, Buzgo M, Daňková J, Litvinec A, Vocetková K, Plencner M. The combination of nanofibrous and microfibrous materials for enhancement of cell

infiltration and in vivo bone tissue formation. *Biomedical Materials*. 2018; 13: 025004. Available from: https://doi.org/10.1088/1748-605X/aa9717.
[17] Hadida M, Marchat D. Strategy for achieving standardized bone models. *Biotechnology and Bioengineering*. 2020; 117: 251-271. Available from: https://doi.org/10.1002/bit.27171.
[18] Yu D, Wang J, Qian KJ, Yu J, Zhu HY. Effects of nanofibers on mesenchymal stem cells: environmental factors affecting cell adhesion and osteogenic differentiation and their mechanisms. *Journal of Zhejiang University - Science B*. 2020; 21: 871-884. Available from: https://doi.org/10.1631/jzus.b2000355.
[19] Gerardo-Nava J, Führmann T, Klinkhammer K, Seiler N, Mey J, Klee D, Möller M, Dalton PD, Brook GA. Human neural cell interactions with orientated electrospun nanofibers in vitro. *Nanomedicine*. 2009; 4: 11-30. Available from: https://doi.org/10.2217/17435889.4.1.11.
[20] Sikavitsas VI, Bancroft GN, Holtorf HL, Jansen JA, Mikos AG. Mineralized matrix deposition by marrow stromal osteoblasts in 3D perfusion culture increases with increasing fluid shear forces. *Proceedings of the national academy of sciences*. 2003; 100: 14683. Available from: https://doi.org/10.1073/pnas.2434367100.
[21] Su WT, Wang YT, Chou C.-M. Optimal fluid flow enhanced mineralization of MG-63 cells in porous chitosan scaffold. *Journal of the Taiwan Institute of Chemical Engineering*. 2014; 45: 1111-1118. Available from: https://doi.org/10.1016/j.jtice.2013.10.016.
[22] Gomes ME, Bossano CM, Johnston CM, Reis RL, Mikos AG. In Vitro Localization of Bone Growth Factors in Constructs of Biodegradable Scaffolds Seeded with Marrow Stromal Cells and Cultured in a Flow Perfusion Bioreactor. *Tissue Engineering*. 2006; 12: 177-188. Available from: https://doi.org/10.1089/ten.2006.12.177.
[23] Du D, Furukawa KS, Ushida T. 3D culture of osteoblast-like cells by unidirectional or oscillatory flow for bone tissue engineering. *Biotechnology and Bioengineering*. 2008; 102: 1670-1678. Available from: https://doi.org/10.1002/bit.22214.
[24] Fassina L, Visai L, Asti L, Benazzo F, Speziale P, Tanzi M, Magenes G. Calcified Matrix Production by SAOS-2 Cells Inside a Polyurethane Porous Scaffold, Using a Perfusion Bioreactor. *Tissue Engineering*. 2005; 11: 685-700. Available from: https://doi.org/10.1089/ten.2005.11.685.
[25] Abo-Aziza FA, Zaki AA. The Impact of Confluence on Bone Marrow Mesenchymal Stem (BMMSC) Proliferation and Osteogenic Differentiation. *International Journal of Hematology-Oncology and Stem Cell Research*. 2017; 11: 121.
[26] Kim SS, Sundback CA, Kaihara S, Benvenuto MS, Kim BS, Mooney DJ, Vacanti JP. Dynamic Seeding and in Vitro Culture of Hepatocytes in a Flow Perfusion System. *Tissue Engineering*. 2000; 6: 39-44. Available from: https://doi.org/10.1089/107632700320874.
[27] Koch MA, Vrij EJ, Engel E, Planell JA, Lacroix D. Perfusion cell seeding on large porous PLA/calcium phosphate composite scaffolds in a perfusion bioreactor system under varying perfusion parameters. *Journal of Biomedical Materials Reserach*. 2010; 95A: 1011-1018. Available from: https://doi.org/10.1002/jbm.a.32927.
[28] Zhao F, Ma T. Perfusion bioreactor system for human mesenchymal stem cell tissue engineering: Dynamic cell seeding and construct development. *Biotechnology and Bioengineering*. 2005; 91: 482-493. Available from: https://doi.org/10.1002/bit.20532.
[29] Dar A, Shachar M, Leor J, Cohen S. Optimization of cardiac cell seeding and distribution in 3D porous alginate scaffolds. *Biotechnology and Bioengineering*. 2002; 80: 305-312. Available from: https://doi.org/10.1002/bit.10372.
[30] Gao J, Niklason L, Langer R. Surface hydrolysis of poly(glycolic acid) meshes increases the seeding density of vascular smooth muscle cells. *Journal of Biomedical Materials Research*. 1998; 42: 417-724. Available from: https://doi.org/10.1002/(SICI)1097-4636(19981205)42:3%3C417::AID-JBM11%3E3.0.CO;2-D.
[31] Kim BS, Putnam AJ, Kulik TJ, Mooney DJ. Optimizing seeding and culture methods to engineer smooth muscle tissue on biodegradable polymer matrices. *Biotechnology and Bioengineering*. 1998; 57: 46-54. Available from: https://doi.org/10.1002/(SICI)1097-0290(19980105)57:1%3C46::AID-BIT6%3E3.0.CO;2-V
[32] Saini S, Wick TM. Concentric Cylinder Bioreactor for Production of Tissue Engineered Cartilage: Effect of Seeding Density and Hydrodynamic Loading on Construct Development. *Biotechnology Progress*. 2003; 19: 510-521. Available from: https://doi.org/10.1021/bp0256519.
[33] Olivier V, Hivart P, Descamps M, Hardouin P. In vitro culture of large bone substitutes in a new bioreactor: importance of the flow direction. *Biomedical Materials*. 2007; 2: 174-180. Available from: https://doi.org/10.1088/1748-6041/2/3/002.